Solvation and Ion-Pairing Properties of the Aqueous Sulfate Anion: Explicit versus Effective Electronic Polarization

Luís Pegado,[a], Ondrej Marsalek,[b], Pavel Jungwirth[b] and Erik Wernersson*[b]

[a] *Laboratory for Waste Management, Paul Scherrer Institute, 5232 Villigen PSI, Switzerland,* [b] *Institute of Organic Chemistry and Biochemistry, Academy of Sciences of the Czech Republic, Flemingovo nám. 2, CZ-16610 Prague 6, Czech Republic*

**E-mail: erik.wernersson@fkem1.lu.se, Present Address: Physical Chemistry, Department of Chemistry, Lund University, P.O. Box 124, SE-22100 Lund, Sweden*

Received Xth XXXXXXXXXX 20XX, Accepted Xth XXXXXXXXX 20XX

First published on the web Xth XXXXXXXXXX 200X

DOI: 10.1039/b000000x

Abstract

We assessed the relative merits of two approaches for including polarization effects in classical force fields for the sulfate anion. One of the approaches is the explicit shell model for atomic polarization and the other is an implicit dielectric continuum representation of the electronic polarization, wherein the polarizability density is spatially uniform. Both the solvation and ion association properties of sulfate were considered. We carried out an ab initio molecular dynamics simulation for a single sulfate anion in aqueous solution to obtain a benchmark for the solvation structure. For the ion-pairing properties, the models were compared to experimental thermodynamic data through Kirkwood-Buff theory, which relates the integrals of the pair correlation functions to measurable properties. While deficiencies were found for both of the approaches, the continuum polarization model was not systematically worse than the shell model. The shell model was found to give a more structured solution than the continuum polarization model, both with respect to solvation and ion pairing.

1 Introduction

Sulfate salts are important in many technical, biological, and environmental contexts. The sulfate ion is strongly hydrated, as indicated by its large negative entropy of solvation,[1] and occupies a position near the salting-out end of the Hofmeister series.[2] This is illustrated clearly by cold denaturation experiments on elastin-like peptides, in which the effect of various sodium salts on the lower consolute temperature was found to correlate directly with the entropy of hydration of the anion.[3] The ion specificity of phase equilibria of biomolecules in salt solution is exploited to grow protein crystals for X-ray and neutron crystallography. Particularly ammonium sulfate is an efficient protein crystallizing agent. A survey of 650 protein database entries indicates that it is the most commonly used salt precipitant.[4] For this reason, an accurate model of the sulfate ion is essential to, for instance, accurately describe protein crystals incorporating ammonium sulfate-containing buffer solution, as was attempted in ref[5].

The description of salts containing divalent oxyanions using non-polarizable force fields appears to be problematic. Few simulations of salts containing such anions together with small or polar cations are reported in the literature. In those that exist, the typical behavior is extensive ion aggregation.[5–7] In the specific case of sodium sulfate, there is excessive ion aggregation for a range of sulfate force field parameters, but this behavior was not encountered for polarizable models.[8] For these, a reasonable solution structure was obtained, which was roughly consistent with experimental chemical potential data.[8] The qualitatively different behaviors of polarizable and non-polarizable models was attributed to the polarization of the first solvation shell of sulfate, which stabilizes it and tends to suppress contact ion-pairing.[8]

The balance between solvation and ion pairing is important for the structure and properties of electrolytes in general, and the difficulties encountered in describing sulfate salt solutions suggest that this balance is especially precarious for systems containing multivalent ions. To investigate the solvation structure of the sulfate ion, we performed an ab initio molecular dynamics (AIMD) simulation of a single sulfate ion in water. This simulation was used as a benchmark to assess the performance of force field models, with the ultimate aim of finding a

simple model that gives acceptable descriptions of both solvation structure and ion association. We also assess the performance of force field models with respect to ion association in salt solutions by comparing to experimental thermodynamic data. This is done via Kirkwood-Buff (KB) theory,[9,10] which relates the radial distribution functions to experimentally accessible quantities such as the partial molar volumes and the concentration derivatives of the chemical potential.

Special emphasis is placed on the treatment of polarization effects in the force field models. We compare a shell model (SM)[11] of electronic polarization to an 'electronic continuum correction' (ECC) model, treating such polarization effectively in terms of a dielectric continuum, as suggested in a recent series of papers.[12–15] It is important to note that these two approaches are based on different physical assumptions, the latter is not merely an approximation to the former. In a SM, the polarization is assumed to be localized in the vicinity of the atomic sites. In ECC models, however, an assumption that the electronic polarizability density is uniform in space, and similar to that on the macroscopic scale, is implicit in the ansatz of dielectric continuum-like polarization. It is a priori not obvious which of these extremes is closer to reality on the molecular scale. ECC models have been constructed for water as well as for polar organic solvents.[13,16] This approach has also been applied to model potassium carbonate and nitrate solutions, and gives a good account of the difference in structure factors between such solutions measured by neutron scattering.[17]

It is found here that the ECC model is comparable to, and in some important respects preferable to, the SM, which, as expected, is found to be similar to point polarizable models, both with respect to the sulfate solvation structure and the sodium sulfate solution properties. This result is qualitatively robust with respect to moderate changes in the sulfate force field parameters.

2 Simulation Methods

We consider two types of systems: a single sulfate ion in aqueous solution and solutions of sodium sulfate. The former type of system is treated by both ab initio and force field molecular dynamics simulations, while for the latter only force field models are used.

2.1 Ab Initio Simulations

While AIMD simulations have the potential for giving a more accurate picture of molecular structure and dynamics than force field simulations, it is not guaranteed that this potential will be realized for any given combination of method and system. The description of aqueous solvation by electronic structure methods, typically density functional theory (DFT), has been hampered by the fact that many density functionals give a poor description of liquid water.[18] It has been shown recently, however, that the situation can be greatly improved by introducing empirical corrections to include dispersion interactions.[19,20] An electronic structure method that describes water-water interactions well can be expected to also perform well for the sulfate-water interactions, that are dominated by oxygen-oxygen and hydrogen-oxygen interactions. For this reason, we consider it justified to use the AIMD simulations described below as a benchmark for the solvation structure of sulfate.

Born-Oppenheimer AIMD simulations were performed using the CP2K simulation package.[21] The simulated system contained 64 water molecules and one sulfate ion. The periodic simulation cell was cubic, with an edge length of 12.41 Å. The net negative charge of the system was canceled by introducing a uniform, positive charge density. We used the Becke correlation functional[22] together with the Lee-Yang-Parr exchange functional[23] and the second-generation Grimme dispersion correction (BLYP-D2).[24] The Kohn-Sham orbitals were expanded in a triple-zeta valence Gaussian basis set with two additional polarization functions, optimized for condensed molecular systems (molopt-TZV2P).[25] The Goedecker-Teter-Hutter norm-conserving pseudopotentials were used on all atoms,[26] and replaced the core electrons of oxygen and sulfur. The electron density was represented using plane waves with a cut-off of 280 Ry. The self-consistent field cycle was converged to within one part per million each 0.5 fs time step. A temperature of 300 K was imposed using a velocity rescaling thermostat with a time constant of 50 fs.[27]

Initial configurations were obtained from a classical molecular dynamics simulation with the sulfate force field recommended in ref[8] and POL3[28] water. The simulation setup was the same as that in ref[8], except that the cut-off for non-bonded interactions was reduced to 5.0 Å and that the volume was held constant. The dimensions of the cell were determined from a simulation at constant pressure. The force field calculations were performed using the AMBER10 program package.[29]

Five independent AIMD trajectories were simulated. The initial portion of each trajectory, roughly 5 ps, was discarded as equilibration of the transition from the empirical force field. This equilibration was monitored through the convergence of the system energy. A total of 52.5 ps of production data was collected. The electron density of the system was saved on the full resolution grid with dimensions of 125x125x125 points every 10 steps. This density was then decomposed into molecular charges using Bader population analysis,[30] as implemented in ref[31]. Although atomic populations would be desirable for comparison with the force field partial charges, see below, such populations could not be calculated reliably due to the use of pseudopotentials. We also calculated the dipole moments of the water molecules, using maximally lo-

Distances		r_0(Å)	k_S (kJ/mol/Å^2)
S-O		1.5247	
O-O		2.4898	
O-Os		0	3130.9
Non-Bonded Parameters	σ (Å)	ε (kJ/mol)	Charge (e$_0$)
S	3.55	1.046	2.0
O	3.15	0.8368	-1.0 (-3.0^a)
Os	0	0	2.0

^{a} For the SM.

Table 1 Force field parameters for the sulfate ion, "Os" refers to the shell particles for the oxygen atoms in the SM.

calized Wannier functions.[32]

2.2 Force Field Simulations

The force field parameters for sulfate are shown in Table 1. We also carried out simulations for selected variations of the model parameters to test the sensitivity of the results to the details of the force field, as noted below. This sulfate model is based on an existing non-polarizable model,[33] which is also basis of the polarizable model recommended in ref.[8]. Two fundamentally distinct ways of treating atomic polarizability were considered, namely the SM and ECC approaches mentioned in the Introduction. Lorentz-Berthelot combination rules are employed throughout for the Lennard-Jones parameters.

In the SM approach, polarization is treated by affixing charged shell particles to atomic sites by harmonic restraints. For sulfate, shell particles were assigned to the oxygens only. The shell charge was 2 e_0, with the oxygen partial charge made more negative by the corresponding amount, and the spring constant k_S was chosen to correspond to a point polarizability of 1.775 Å^3 for each oxygen, consistent with the sulfate polarizability obtained from ab initio calculations.[34] Due to the polarization catastrophe,[35] the polarizability of the oxygen atoms in a previous variant of this model using point-dipole polarizabilities, see ref.[8], was assigned a value of 1 Å^3. We found that in the SM, the polarization catastrophe could be avoided by using positive shell charges. The physical explanation for this difference is that a shell of opposite charge to that of its corresponding atom will typically be repelled by the instantaneous reaction field from the surrounding solution. As the shells then tend to be displaced towards a region of weaker electric field, the polarization catastrophe is less likely to occur than in the opposite situation. This is the reason for replacing the point polarizable model with a SM, which has similar, but evidently not identical, properties. A SM polarizable water model, SWM4-NDP,[36] was used in combination with the SM sulfate. The fact that this water model has a dielectric constant close to the experimental one makes it especially suitable for simulations of aqueous electrolyte solutions. An additional advantage is that a model of the sodium ion parametrized specifically for this water model exists.[37]

In the ECC approach, electronic polarization effects are taken into account, in a mean-field way, via a dielectric continuum.[15] With respect to the forces between atoms, the screening from this electronic dielectric continuum is equivalent to a scaling of all charges by a factor of $1/\sqrt{\varepsilon_e}$, where ε_e is the electronic part of the relative permittivity. Note, however, that the assumption of an electronic dielectric continuum has implications for the solvation free energy, to which a self-energy given by the Born expression has to be added. As argued in ref.[15], the most appropriate choice of ε_e is the optical dielectric constant of the material in question. In the ECC model considered here, ε_e was set to 1.78, the value appropriate for pure water.[1] Together with the ECC model for sulfate, we employed the TIP4P/2005 water model, which is parametrized to reproduce the experimental region of the phase diagram pertinent to the various ice phases.[38] The partial charges of the water molecule were *not* scaled, as these were taken as fitting parameters in the construction of the water model. Therefore, they should be regarded as effective charges, already taking electronic polarization into account.[13,15]

2.2.1 Solvation of a Single Sulfate Ion The system composition and volume were identical to those for the AIMD simulations described above. Long range electrostatic interactions were taken into account using the particle-mesh Ewald method with a grid spacing up to 1.2 Å. As in the AIMD simulations, the negative charge of the system was canceled by a uniform background charge density. The temperature was kept constant at 300 K using the canonical velocity rescaling thermostat.[27] The sulfate geometry was kept rigid using the SHAKE algorithm.[39] The cut-off for short range, Lennard-Jones and real-space Coulomb, interactions was 5 Å. To investigate the effect of the small system size and short cut-off distance, a system with one sulfate ion and 512 water molecules was also considered. For this system, the cut-off distance was 9 Å and the calculations were done at constant pressure of 1 bar using the weak coupling barostat.[40] With respect to the sulfate solvation structure, only minor quantitative differences were found between the system sizes. The calculations were carried out using the GROMACS program package, version 4.5.4.[41]

2.2.2 Sodium Sulfate Solutions Three system compositions were considered, containing 27, 54, and 89 formula units of sodium sulfate and 2964, 2834, and 2601 water molecules, respectively. This corresponds to salt concentrations of approximately 0.5, 1.1, and 1.9 m. The force field parameters from ref.[37] were used for sodium cations for the SM simulations. For the ECC simulations, this model was modified by removing the polarizability and scaling the charge by the

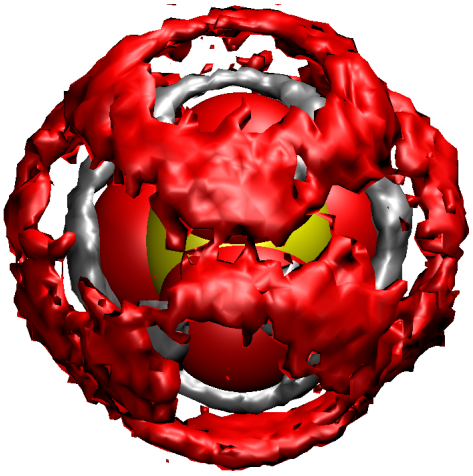

Fig. 1 Isodensity surfaces for oxygen (red) and hydrogen (gray), corresponding to the first solvation shell of the sulfate ion. The isovalue is twice the average concentration in the simulation box.

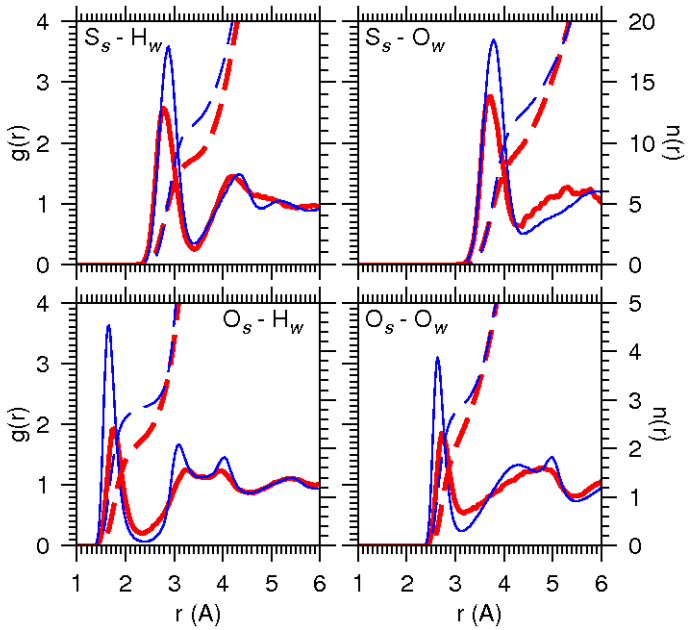

Fig. 2 Radial distribution functions for the pairs of atom types indicated (full curves, left axis) and cumulative numbers (dashed lines, right axis). The thick red lines are from AIMD simulations and the thin blue lines are for the classical simulation used to generate the initial configurations.

appropriate factor, see above. We note, however, that the Lennard-Jones parameters should, in general, be re-optimized to construct an optimal ECC model. The simulation setup was similar to that for the individual ions except that the cut-off for short range interactions was 9.0 Å and the simulations were carried out at constant pressure of 1 bar.

3 Results

3.1 Ab Initio Simulation

The isodensity surfaces for water oxygen and hydrogen in the vicinity of a sulfate ion obtained from the AIMD simulation are shown in Figure 1. Both form rings around the sulfate oxygens, the hydrogen contours narrower and closer than the oxygen contours. This corresponds to a tetrahedral arrangement of water molecules that donate hydrogen bonds to the sulfate oxygens, consistent with force field simulations.[8,33]

In Figure 2 the radial distribution functions from the AIMD simulation are shown, together with the corresponding radial distribution functions for the polarizable empirical model used in ref.[8]. The empirical model has a significantly more structured solvation shell, as indicated by the larger first peaks in each of the radial distribution functions. The difference in peak height between the AIMD and force field simulations is the greatest for the radial distribution functions pertaining to the sulfate oxygens.

The coordination number for water oxygen around the sulfate sulfur and water hydrogen around each of the sulfate oxygens are 9.4 and 2.1, respectively, in the AIMD simulations. For the purpose of this discussion, these coordination numbers are defined as the number of solvent atoms within 4.3 Å and 2.3 Å of the respective solute atom, which correspond to the approximate positions of the first minima of the relevant radial distribution functions. For the force field simulation, the corresponding numbers evaluated for the same cut-off distances are 12.1 and 2.8. Thus, the typical number of hydrogen bonds to each of the sulfate oxygens is close to two in the AIMD simulation while the force field model predicts a number closer to three. While the solvation structure is qualitatively similar between the AIMD and force field calculations, the latter displays significantly stronger hydration.

Bader population analysis for the sulfate gives a total charge in a narrow distribution around -1.62 e_0, with a standard deviation of 0.02 e_0. It has been noted previously that the Bader charge of chloride in water obtained from ab initio calculations does not correspond to the nominal charge, but to approximately -0.8 e_0.[42] Thus, the relative change compared to the nominal charge is very similar between chloride and sulfate. The Bader charges on the water molecules were also calculated, to discern where the electron density shed by the sulfate ion is located. It was found that each water molecule had an excess charge of approximately -0.006 e_0. Interestingly, the water partial charge was largely uncorrelated to the distance from the sulfate ion. The excess electron density thus appears to be approximately evenly distributed over the water molecules in the simulation box, rather than concentrated

	S_s-O_w		O_s-H_w	
	SM	ECC	SM	ECC
original	12.32	10.55	2.92	2.33
q_O -20%	11.78	10.04	2.84	2.27
q_O +20%	12.66	10.97	2.95	2.40
σ_O -5%	12.55	11.03	2.93	2.44
σ_O +5%	11.98	9.81	2.88	2.15

Table 2 Coordination numbers for different variants of the sulfate model. The cut-offs are 4.3 and 2.3 Å for the S_s-O_w and O_s-H_w coordination, respectively.

to the first solvation shell as one might intuitively expect. To determine whether this was an artifact of either the absence of explicit counterions or insufficient system size, single point calculations were performed on configurations from the (0.5 m) salt system. These calculations resulted in similar values of the sulfate charges and sodium charges of around 0.9 e_0, with the remaining excess negative charge still located on the water molecules. Thus, the reduction of the sulfate charge is a true feature of the underlying model, as opposed to a feature of the calculation set-up, but the almost even distribution of the excess charge over water molecules appears to be due to the absence of counterions.

The average dipole moment of the water molecules was 3.1 D with a standard deviation of 0.3 D. No statistically meaningful dependence on the distance to the sulfate ion was detected. The sampling, however, was not sufficient to either confirm or refute the structure seen in the dipole moment profile from force field simulations, see ref[8] and the SI.

3.2 Reproduction of the Solvation Structure By Force Field Models

To investigate the sensitivity of the sulfate solvation structure to the force field parameters, we considered a limited set of parameter variations around the values given in Table 1. These consisted of 5% increase or decrease in the oxygen Lennard-Jones size parameter σ_O and a 20 % increase and decrease in the oxygen partial charges, with the corresponding change in the sulfur partial charge to maintain the total charge. A halving and doubling of ε_O was also considered, but was found to have an effect very similar to that of the variation in σ_O. Apparently, the effect of the variation of ε_O on the softness of the repulsive part of the Lennard-Jones potential has concequences similar to those of a change in the oxygen size embodied by σ_O. Oxygen polarizability of 1 Å^3, same as in ref[8], was also considered for the SM sulfate, but the change had only minor structural consequences. For this reason, only the variations in σ_O and q_O are discussed in detail below.

The effect of the parameter variations on the coordination numbers are shown in Table 2. The cut-offs are 4.3 and 2.3 Å, respectively, the same as for the AIMD coordination numbers. Note that the actual minima of the corresponding radial distribution functions are not located exactly at these positions, see Figures 3 and 4 below. For the SM sulfate, the S_s-O_w and O_s-H_w coordination numbers are around 12 and 2.9, respectively, in all cases. These are in line with the values from the point-polarizable model and thus significantly larger than the values from the AIMD simulation. The ECC model shows a slightly broader variation in coordination numbers, with typical values being around 10-11 for the S_s-O_w coordination number and 2.2-2.4 for the O_s-H_w coordination number. The minima of the corresponding radial distribution functions occur at larger r for all the force field variants than for the AIMD. Using the actual minimum position for each force field variation would, therefore, result in higher coordination numbers.

The variation of the radial distribution functions with the oxygen partial charges and sizes for the SM sulfate in the region around the first peak is shown in Figure 3. Increasing the magnitude of q_O or decreasing σ_O exasperates the overstructuring seen in Figure 2. Increasing σ_O brings the peak heights more in line with those from the AIMD simulations, but worsens the agreement between between the peak positions for the radial distribution functions involving S_s. The agreement with the AIMD simulation appears conspicuously better, however, for the model with reduced magnitude of q_O. The height and position of the first peak in the S_s-H_w radial distribution functions is well reproduced by the model with less negative oxygen partial charges, but the first minimum thereafter is better reproduced by the model with more negative oxygens. With respect to the first peak, the trend in the S_s-O_w radial distribution function is similar. The heights of the first peaks in both the O_s-O_w and O_s-H_w are also best reproduced by the model with the least negative oxygen partial charges. The large difference in the first peak height of radial distribution functions can be reconciled with the smaller difference in the coordination numbers, see Table 2, by noting that the peak narrows with increasing negative oxygen charge. While both the peak positions and heights are improved by reducing the magnitude of the oxygen partial charges, the solvation shell of this sulfate model variant still contains a too large number of water molecules overall.

In Figure 4, the effect of varying the oxygen size and partial charge on the radial distribution functions is shown for the ECC sulfate. Although the trends are similar to those for the SM sulfate, the magnitude of the variations are smaller. The peak heights are systematically smaller than for the SM sulfate and the typical agreement of the peak heights with the AIMD radial distribution functions is better. This is especially true for the O_s-O_w and O_s-H_w radial distribution functions. In contrast to the situation for the SM model, it does not appear to be possible to improve the agreement significantly by varying the

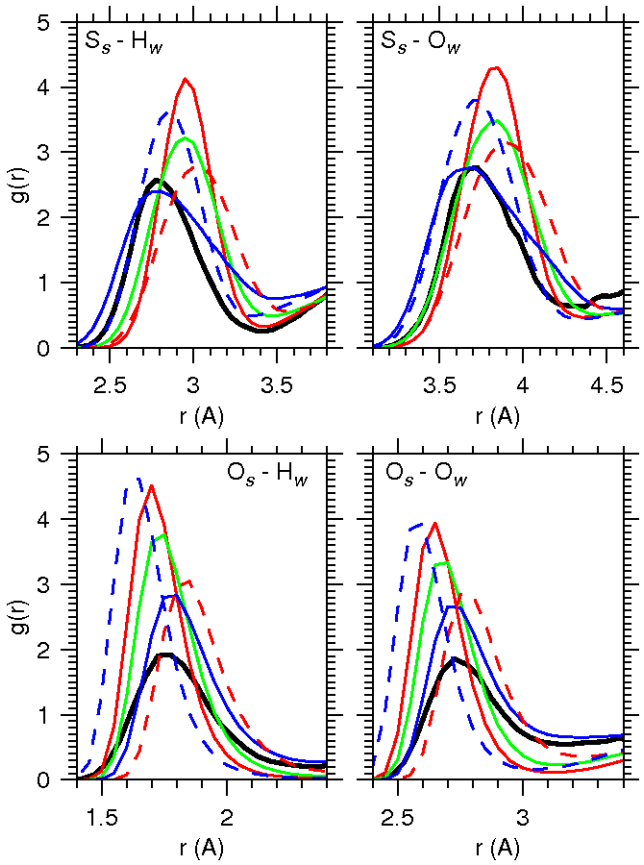

Fig. 3 First peaks of the sulfate water radial distribution functions for the atoms indicated from the AIMD simulation (black curves), the SM version of the sulfate force field presented in Table 1 (green curves) and variations of this model: Full curves correspond to a 20% increase (red) and decrease (blue) in the magnitude of q_O and dashed curves correspond to a 5% increase (red) and decrease (blue) in σ_O.

oxygen partial charge only: Making the oxygen less negative improves the position of the first peak of the S_s-O_w radial distribution function but deteriorates the agreement with respect to both shape and height. Overall, however, the agreement with the AIMD simulation is better than for the SM sulfate model.

To assess the effect of the charge scaling in itself, as opposed to differences in the water model, a model identical to the ECC sulfate in every way except that the charges are not scaled was investigated, see Figure 5. The solvation structure was broadly similar to that for the SM model, which is remarkable. Due to the fact that the SM model contains electronic polarization explicitly, one would rather expect that the SM and ECC models would be mutually similar and different from the non-polarizable model. Possible reasons for this observation will be discussed below.

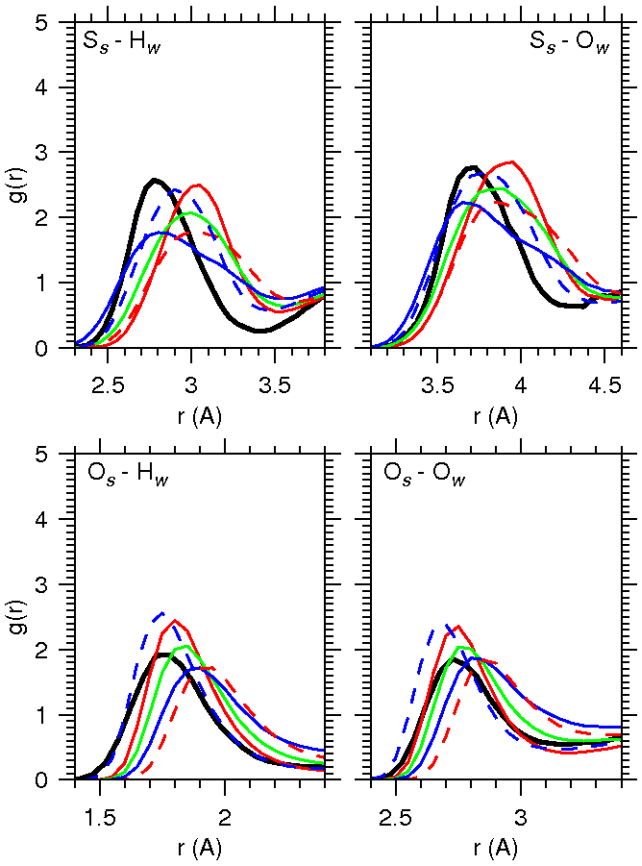

Fig. 4 Same as Figure 3 but for an ECC version of the sulfate model.

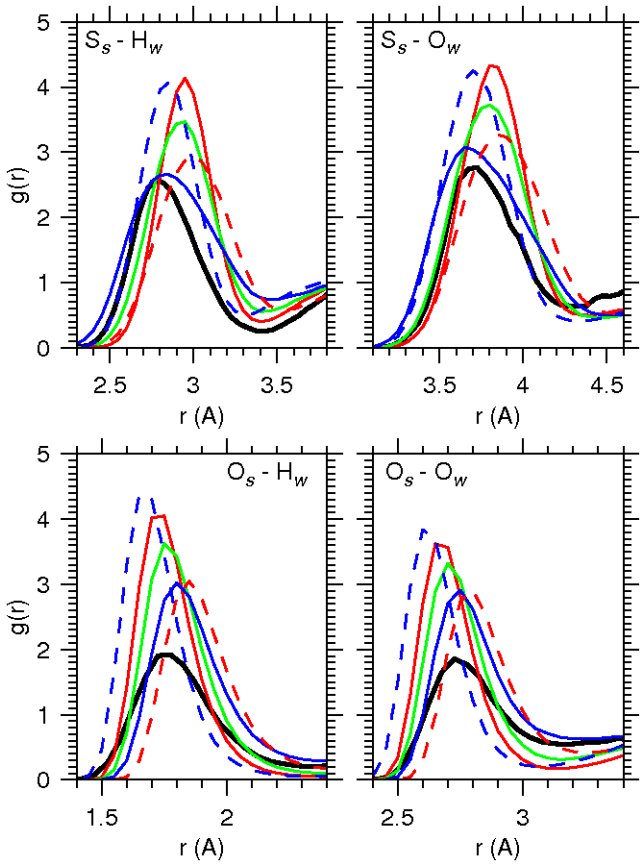

Fig. 5 Same as Figure 4, but with the full ionic charges.

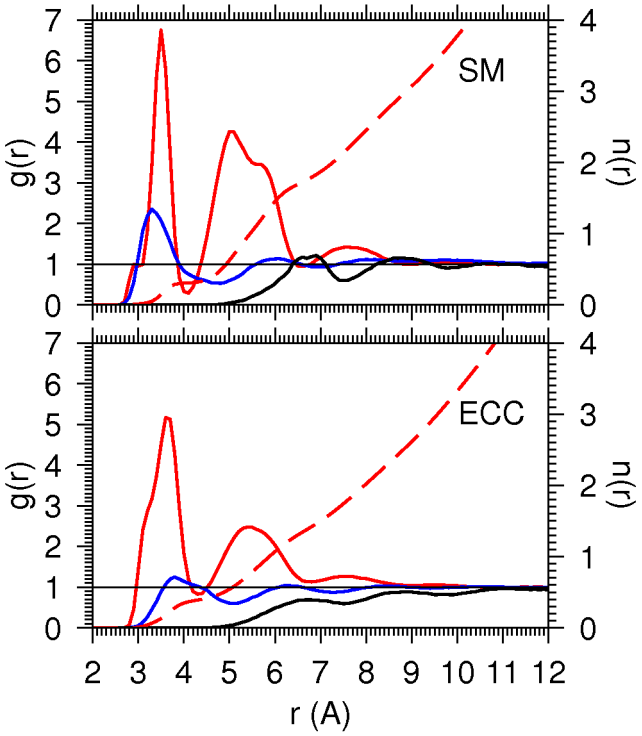

Fig. 6 Radial distribution functions for 0.5 m sodium sulfate solutions with the SM and ECC sulfate models. Red, blue and black curves are for the, S_s-Na, Na-Na and S_s-S_s radial distribution functions, respectively. The dashed lines show the cumulative numbers of Na^+ ions around S_s, right axis.

The induced dipole moments of the water molecules as a function of distance to the sulfate ion were calculated for the SM sulfate model variants and the results are shown in the SI. Although notable differences were found, the qualitative feature that the first solvation shell was more polarized than the bulk, seen in ref[8], was retained in all model variants.

3.3 Salt solutions

Simulations of salt solutions using the SM sulfate were performed with both the force field variant in Table 1 and the variant where q_O was reduced by 20%. The former model was found to be similar to the polarizable model in ref.[8]. The latter model formed aggregates similar to those seen for non-polarizable models of sodium sulfate solutions in that work. We also tried a model with a 10% reduction in $|q_O|$, to investigate what oxygen partial charges are needed for a soluble sodium sulfate model, and this model also gave rise to cluster formation. A polarizable water model is thus not sufficient to guarantee the solubility of sodium sulfate for all combinations of force field parameters within the physically reasonable space, and the model considered here appears to be close

	N_{cc}	N_{cw}	Γ	ρ (g/cm^3)
0.5 m				
SM	1.16	-0.60	0.73	1.067
ECC	0.34	-0.87	0.45	1.051
exp	0.55	-0.64	0.52	1.057
1.1 m				
SM	2.51	-1.54	1.20	1.134
ECC	0.44	-1.03	0.50	1.105
exp	0.61	-0.87	0.55	1.123
1.9 m				
SM	2.70	-2.02	1.30	1.228
ECC	0.46	-1.23	0.53	1.179
exp	0.33	-0.91	0.48	1.212

Table 3 Kirkwood-Buff excess coordination numbers. The estimated error in N_{cc} and N_{cw} is typically within 0.1 and that in Γ is within 0.05 as determined by block averages. For the SM model at the higher concentrations the error is larger: 0.5 for N_{cc}, 0.3 for N_{cw} and 0.2 for Γ.

to the border between clustering and non-clustering models.

The radial distribution functions for sodium sulfate solutions with the SM and ECC sulfate models are shown in Figure 6. There is a larger degree of ion association for the SM than for the ECC, as can be seen most clearly from the S_s-*Na* radial distribution function and the corresponding cumulative numbers. For both force fields, there are three well separated peaks in the S_s-*Na* radial distribution function. The first and second peaks correspond, respectively, to contact ion pairs and solvent-shared ion pairs. The third peak, which is much less pronounced, can be described as corresponding to solvent-separated ion pairs. Both the first and second peaks have a shape that suggests some internal structure. For the first peak, the shoulder at small r corresponds to bidentate contact pairs, while the main peak is composed of monodentate contact pairs, see SI.

As can be seen from the cumulative numbers, the first peak in the S_s-*Na* radial distribution function for the SM sulfate contains fewer ions than the corresponding peak for the ECC sulfate, though it is higher. The difference in the second peak is greater, a fact that can be seen clearly from both the radial distribution functions and the cumulative numbers. The like-ion radial distribution functions are qualitatively similar between the SM and ECC sulfate solutions, but show greater structure in the former case.

The radial distribution functions can be related to experimental partial molar volumes and the concentration dependence of the chemical potential through the Kirkwood-Buff (KB) integrals, G_{ij}

$$G_{ij} = 4\pi \int_0^\infty (g_{ij}(r) - 1) r^2 dr, \qquad (1)$$

which can be deduced from measurements of those properties.[9] Note that the salt has to be formally treated as a single chemical species due to the electroneutrality condition.[10] For a binary electrolyte, all relations become formally equivalent to those for a neutral compound if all ions are treated as indistinguishable.[43] This convention is adopted here. In Table 3, the KB integrals implied by the simulated radial distribution functions are shown and compared to the experimental values, in terms of the dimensionless quantities $N_{cc} = n_c G_{cc} = n_c G_{+-} - 1$ and $N_{cw} = n_w G_{cw}$, where index c denotes "solute" ("c" for co-solute) and w denotes "water", and $n_c = n_+ + n_-$ is the total concentration of ions. N_{cc} and N_{cw} are to be interpreted as the excess number of water molecules and ions, respectively, in the vicinity of any ion. See SI for a complete discussion and the details of the procedure by which the KB integrals were calculated from experimental data. Also the mass density, ρ, and the parameter Γ, related to the *molar* activity derivative according to

$$\frac{\partial \ln a_c}{\partial \ln n_c} = \frac{1}{1 + N_{cc} - \frac{n_c}{n_w} N_{cw}} = \frac{1}{\nu \Gamma}, \qquad (2)$$

where ν is the number of ions in a formula unit, are presented in Table 3.

The SM consistently gives a too large value for N_{cc}, while the ECC model typically gives slightly too small values. Thus, the former model overestimates and the latter underestimates ion association. This is also reflected in Γ in both cases. Note that the qualitatively similar radial distribution functions in Figure 6 give very different values of N_{cc}. This illustrates that this quantity is a sensitive measure of association in salt solutions. For N_{cw}, both the ECC and SM models tend to give a too negative value, though the SM model at 0.5 m concentration, which agrees with experiment within the simulation error, is a notable exception. The ECC and SM predict densities on opposite sides of the experimental value.

Several variants of the ECC model were also considered, as this could be achieved at moderate computational cost, and show relatively moderate differences in N_{cc} and N_{cw}, as discussed in detail in the SI. The exception is the variant with reduced $|q_O|$, which gives a significantly larger value of N_{cc}, around 0.64. This can be ascribed to an increased propensity to form "bidentate" ion pairs, where the sodium ions are located between the oxygen atoms, as the sulfur becomes less positive. This observation also gives a hint towards why the corresponding SM sulfate model variant shows clustering, as the same mechanism should be present in the polarizable model.

The present results for the SM sulfate are consistent with the results in ref[8], which reports Γ at 0.5 m for two water models as 0.53 and 0.71. This indicates that the behavior of sulfate in polarizable water models is robust. The SM sulfate, however, overestimates ion association at high concentration, though it

does not give rise to the irreversible cluster formation seen for non-polarizable models. It is important to note that N_{cc} and N_{cw} are not independent quantities; a larger number of ions in the vicinity of any given ion will displace water molecules and make N_{cw} more negative than for a less strongly associated salt with the same solvation properties. Thus, it would be an error to conclude that a model variant with N_{cw} close to the experimental value describes solvation realistically if a similar agreement is not seen for N_{cc}.

4 Discussion

The SM variants consistently overestimated the coordination number of water around sulfate. Furthermore, a too large degree of association is seen in salt solutions. Particularly, the SM sulfate with the best solvation structure does not give rise to a soluble sodium sulfate model. The ECC model variants give solvation structures closer to that from the AIMD simulations. The ECC models, except for the variant with reduced magnitude of the oxygen partial charges, see SI, underestimate the degree of ion association. This is probably unavoidable with existing water models, as the ECC approach effectively entails scaling up the solvent dielectric constant by ε_e.[15] A water model that has a "good" dielectric constant for use in non-polarizable models will therefore, by that very fact, be inappropriate for use in ECC models.

The dielectric constant of TIP4P/2005 water is around 60,[38] and, therefore, the effective dielectric constant in the ECC model is around 107, compared to the experimental value of around 80. The average of long-range electrostatic interactions between ions in the present ECC model are thus systematically underestimated by about 25%. To resolve this problem, it appears necessary to construct a non-polarizable water model with a dielectric constant of around 45, which would be compatible with ECC models with ε_e taken as the experimental value of the optical dielectric constant, 1.78. Pending the construction of a water model with acceptable dielectric properties when interpreted in the ECC framework, it is hardly meaningful to further refine the ECC sulfate model. In contrast, the SWM4-NDP model reproduces the experimental dielectric constant quantitatively.[36]

The dipole moment of the TIP4P/2005 water model and the reported average dipole moment in liquid phase of the SWM4-NDP water model are similar,[36,38] 2.31 and 2.46 D, respectively. The value obtained from reinterpreting the TIP4P/2005 dipole moment in the ECC framework is 3.07 D,[15] though the assumed dielectric screening actually reduces the strength of the ion-water interactions. It appears likely that the similarity in dipole moment to a large extent explains the similarity between the solvation structure in SWM4-NDP and TIP4P/2005 water with full sulfate charge, which both differ considerably from the TIP4P/2005-based ECC model. The polarizability of the SWM4-NDP model is 0.97825 Å^3,[36] i.e., significantly lower than the experimental gas-phase value of 1.44 Å^3. While the polarizability in condensed phases is not necessarily equal to the gas phase polarizability, the effective polarizability of water molecules in the liquid has been estimated to be similar to the gas phase value, which is also the result obtained from the Clausius-Mossotti relation.[44] Ab initio calculations have given liquid state polarizabilities between 1% larger and 4% smaller than the gas phase value.[45–47] Thus, a reduction by more than 30 %, as assumed in the SWM4-NDP model,[36] appears unlikely. This is not to be confused with the situation for anions, the polarizabilities of which are highly sensitive to the chemical environment.[47–49] The SWM4-NDP water model may in fact give an incomplete treatment of electronic polarization effects, even at the dipole level, and the balance between electronic and nuclear contributions to the response to electric fields is not well reproduced. A similar conclusion about the POL3 model was reached in ref[17].

While the insufficient polarization may be a feature of this particular water model, it may also be indicative of a potential insufficiency of the approximation of SM or point-dipole like polarization for water. The multipole expansion of the atomic polarizability is not guaranteed to converge.[50] Point-polarizable and similar models, such as SMs, are thus not universally applicable. Even in cases where they can in principle be applied, dipole-like polarization is not necessarily sufficient, and may give rise to unphysical behavior. A stark example of such behavior is the polarization catastrophe, where the induced dipoles diverge due to mutual polarization.[35] In some cases, the correct value of the dipole polarizability cannot be used, as it gives rise to this unphysical situation. The deviation from point dipole polarizability-like behavior has been investigated for halide-water complexes in the gas phase.[51] It was found that the point polarizability model overestimated the polarization for small separations. The situation could be improved by using a Thole-type approach,[35] in which a finite spatial extent of the induced charge density is introduced ad hoc.

Charge scaling, which is functionally equivalent to an ECC treatment of polarization, has been applied to ionic liquids, often with good result for both structure and dynamics.[52–55] No explicit assumptions were made about dielectric continuum-like screening. Rather, the scaling factor was used as an adjustable parameter and justified in terms of charge transfer, if at all. In light of the arguments advanced in refs[12–15], charge scaling would appear to be mandatory in models of ionic liquids without explicit polarization. In these systems, there is no high dielectric constant solvent to partially compensate for the effect of neglecting electronic polarization. If dielectric screening on the microscopic scale is indeed similar to the bulk dielectric response, the strength of the electrostatic interaction between ions would thus be overestimated by a factor of

ε_e, typically around two for organic compounds. With respect to the contribution of electrostatic interactions to the Boltzmann factor, neglect of electronic polarization would then be roughly equivalent to cooling a room temperature ionic liquid to cryogenic temperatures.

The Bader charge on sulfate in water was found to be lower than the nominal charge by a factor of about 0.8, which suggests that a considerable degree of charge transfer takes place in the system. Hydrogen bonding between water molecules is associated with a small amount of charge transfer.[56–59] In isotropic bulk water, the average net charge transfer is zero due to symmetry, but if this symmetry is broken (e.g. by the introduction of a solute) a non-zero charge transfer could occur. Assuming that there is charge transfer also between water and the sulfate oxygens, this type of mechanism could explain the reduced sulfate charge seen in the AIMD simulations. The charge scaling in the ECC model, by a factor of 0.75, is similar to the reduction of the sulfate charge found in the AIMD simulation. While the justification in terms of dielectric-like polarization may appear incompatible with the charge transfer picture, we note that the distinction between charge transfer and electronic polarization necessarily becomes blurred in the condensed phase. Thus, a coarse grained description of polarization may well include effects that could reasonably be classified as charge transfer in a more detailed treatment.

In light of these considerations, ECC type models appear to be an attractive alternative to more elaborate models that explicitly include polarization effects, as they appear to permit a simple and reasonably accurate description of the polarization in condensed phases. It is important, however, to recognize the limitations of this type of models. As ECC models constitute a reinterpretation of the meaning of the effective parameters of existing non-polarizable water models, the ECC models inherit the disadvantages of such models. Most conspicuously, this type of model is not directly transferable to states where the local environment of each particle is significantly different from the state at which it was parametrized. This makes modeling of interfaces and phase coexistence problematic. It appears that ECC models are directly applicable to such problems only when the phases are similar with respect to their electronic polarizabilities. Fortunately, this holds to a good approximation for the important case of water/hydrocarbon systems. Other systems such as air-water and water-metal interfaces are more problematic, but could in principle be treated within a dielectric continuum model if the effects of the boundaries between different continua are treated explicitly. Techniques for doing so have been developed within the context of coarse grained simulations.[60]

The success of the ECC model also indicates that the explanation of the difference in association between polarizable and non-polarizable sodium sulfate models in terms of the polarization of the first solvation shell is incomplete.[8] In non-polarizable models, the relative strength of ion-ion interactions to ion-water interactions is systematically higher than in ECC models. The excessive association in non-polarizable models can thus be ascribed to an overestimation of interactions in ion clusters, due to a lack of screening from electronic polarization, similar to the situation in ionic liquids discussed above. As this screening is present in polarizable models, though it may not be captured perfectly by a given parametrization, this feature may contribute to the explanation of the clustering observed for non-polarizable, but not for polarizable, models in ref[8]. This would explain why the ECC approach, like the polarizable model, is capable of producing non-clustering sodium sulfate solutions despite being fundamentally unable to reproduce the excess polarization of water molecules in the first solvation shell of sulfate. Also, this may well be the explanation why the ECC model shows a larger population of contact ion pairs than the SM, see Figure 6, despite that the total population of ion pairs is smaller.

5 Conclusions

We considered two ways of including polarization in force fields for the sulfate ion, namely the SM and ECC approaches where polarization is treated explicitly and implicitly as a dielectric continuum, respectively. The ECC approach consistently gave rise to less structured solutions, both with respect to the solvation structure of a single sulfate ion and the ion association in solution. With respect to the solvation structure, the ECC model gives a degree of structuring commensurable with AIMD simulations while the SM gave rise to a systematically over-structured solvation shell. The ECC model shows too weak ion association in salt solutions while the SM displays too strong ion association, as compared to the experimental Kirkwood-Buff integrals. Given the fact that the ECC model is computationally simpler than the SM, the present results suggest that the former approach may be the method of choice where applicable.

6 Acknowledgments

We thank the Czech Science Foundation (Grant P208/12/G016) for support and prof. Petr Slavíček for brininging the ECC model to our attention. L.P. acknowledges financial support by the SNF, Switzerland under grant number CRSI22_130419/1 and thanks his colleagues at the Institute of Organic Chemistry and Biochemistry for amazing hospitality during his two work stays in Prague. O.M. acknowledges support from the International Max-Planck Research School for Dynamical Processes in Atoms, Molecules and Solids in Dresden. P.J. acknowledges the Academy of Sciences for the Praemium Academie award.

References

1 D. R. Lide (ed.), *Handbook of Chemistry and Physics, 90th ed.*, CRC Press, Boca Ranton, FL, 2010.
2 M. G. Cacache, E. M. Landau and J. J. Ramsden, *Q. Rev. Biophys.*, 1997, **30**, 241–277.
3 Y. Cho, Y. Zhang, T. Christensen, L. B. Sagle, A. Chilkoti and P. S. Cremer, *J. Phys. Chem. B*, 2008, **112**, 13765–13771.
4 S. Radaev, S. Li and P. D. Sun, *Acta Crystallogr. D*, 2006, **62**, 605–612.
5 D. S. Cerutti, I. L. Trong, R. E. Stenkamp and T. P. Lybrand, *Biochemistry*, 2008, **47**, 12065–12077.
6 P. Mason, C. E. Dempsey, G. W. Nielson and J. W. Brady, *J. Phys. Chem. B*, 2005, **109**, 24185–24196.
7 A. A. Chivalo and J. M. Simonson, *Collect. Czech. Chem. Commun.*, 2010, **75**, 405–424.
8 E. Wernersson and P. Jungwirth, *J. Chem. Theory Comput.*, 2010, **6**, 3233.
9 J. G. Kirkwood and F. P. Buff, *J. Chem. Phys.*, 1951, **19**, 774–777.
10 P. G. Kusalik and G. N. Patey, *J. Chem. Phys.*, 1987, **86**, 5110–5116.
11 S. W. Rick and S. J. Stuart, in *Reviews in Computational Chemistry, Volume 18*, John Wiley & Sons, Inc., 2002, pp. 89–146.
12 I. V. Leontyev and A. A. Stuchebrukhov, *J. Chem. Phys.*, 2009, **130**, 085102.
13 I. V. Leontyev and A. A. Stuchebrukhov, *J. Chem. Theory Comput.*, 2010, **6**, 1498–1508.
14 I. V. Leontyev and A. A. Stuchebrukhov, *J. Chem. Theory Comput.*, 2010, **6**, 3153–3161.
15 I. Leontyev and A. Stuchebrukhov, *Phys. Chem. Chem. Phys.*, 2011, **13**, 2613–2626.
16 S. Lee and S. S. Park, *J. Phys. Chem. B*, 2011, **115**, 12571–12576.
17 P. Mason, E. Wernersson and P. Jungwirth, *J. Phys. Chem. B*, 2012, submitted.
18 J. VandeVondele, F. Mohamed, M. Krack, J. Hutter, M. Sprik and M. Parrinello, *J. Chem. Phys.*, 2005, **122**, 014515.
19 S. Grimme, *J. Comp. Chem.*, 2006, **27**, 1787–1799.
20 J. Schmidt, J. VandeVondele, I.-F. W. Kuo, D. Sebastiani, J. I. Siepmann, J. Hutter and C. J. Mundy, *J. Phys. Chem. B*, 2009, **113**, 11959–11964.
21 J. VandeVondele, M. Krack, F. Mohamed, M. Parrinello, T. Chassaing and J. Hutter, *Comput. Phys. Commun.*, 2005, **167**, 103–128.
22 A. D. Becke, *Phys. Rev. A*, 1988, **38**, 3098–3100.
23 C. Lee, W. Yang and R. G. Parr, *Phys. Rev. B*, 1988, **37**, 785–789.
24 S. Grimme, J. Antony, S. Ehrlich and H. Krieg, *J. Chem. Phys.*, 2010, **132**, 154104.
25 J. VandeVondele and J. Hutter, *J. Chem. Phys.*, 2007, **127**, 114105.
26 S. Goedecker, S. Teter and M. Hutter, *Phys. Rev. B*, 1996, **54**, 1703.
27 G. Bussi, D. Donadio and M. Parrinello, *J. Chem. Phys.*, 2007, **126**, 014101.
28 J. W. Caldwell and P. A. Kollman, *J. Phys. Chem.*, 1995, **99**, 6208–6219.
29 D. Case, T. Darden, I. T.E. Cheatham, C. Simmerling, J. Wang, R. Duke, R. Luo, M. Crowley, R.C.Walker, W. Zhang, K. Merz, B. Wang, S. Hayik, A. Roitberg, G. Seabra, I. Kolossváry, K.F.Wong, F. Paesani, J. Vanicek, X.Wu, S. Brozell, T. Steinbrecher, H. Gohlke, L. Yang, C. Tan, J. Mongan, V. Hornak, G. Cui, D. Mathews, M. Seetin, C. Sagui, V. Babin and P. Kollman, *AMBER 10*, 2008.
30 R. F. W. Bader, *Accounts of Chemical Research*, 1985, **18**, 9–15.
31 W. Tang, E. Sanville and G. Henkelman, *J. Phys. Condens. Matter*, 2009, **21**, 084204.
32 G. H. Wannier, *Phys. Rev.*, 1937, **52**, 191–197.
33 W. R. Cannon, B. M. Pettitt and J. A. McCammon, *J. Phys. Chem.*, 1994, **98**, 6225–6230.
34 P. Jungwirth, J. E. Curtis and D. J. Tobias, *Chem. Phys. Lett.*, 2003, **367**, 704–710.
35 B. T. Thole, *Chem. Phys.*, 1981, **59**, 341–350.
36 G. Lamoureux, E. Harder, I. Vorobyov, V. M. Anisimov, B. Roux and A. D. MacKerell, Jr., *Chem. Phys. Lett.*, 2006, **418**, 245–249.
37 H. Yu, T. W. Whitfield, E. Harder, G. Lamoureux, I. Vorobyov, V. M. A. A. D. MacKerell, Jr. and B. Roux, *J. Chem. Phys.*, 2010, **6**, 774–786.
38 J. L. F. Abascal and C. Vega, *J. Chem. Phys.*, 2005, **123**, 234505.
39 J. P. Ryckaert, G. Ciccotti and H. J. C. Berendsen, *J. Comp. Phys.*, 1977, **23**, 327–341.
40 H. J. C. Berendsen, P. J. M. Postma, A. DiNola and J. R. Haak, *J. Chem. Phys.*, 1984, **81**, 3684–3690.
41 B. Hess, C. Kutzner, D. van der Spoel and E. Lindahl, *J. Chem. Theory Comp.*, 2008, **4**, 435–447.
42 Z. Zhao, D. M. Rogers and T. L. Beck, *J. Chem. Phys.*, 2010, **132**, 014502.
43 R. Chitra and P. E. Smith, *J. Phys. Chem. B*, 2002, **106**, 1491–1500.
44 A. V. Grubskaya and P. G. Kusalik, *J. Chem. Phys.*, 2002, **117**, 5290–5302.
45 C. Millot and B. J. C. Cabral, *Chem. Phys. Lett.*, 2008, **460**, 466–469.
46 R. A. Mata, B. J. C. Cabral, C. Millot, K. Coutinho and S. Canuto, *J. Chem. Phys.*, 2009, **130**, 014505.
47 M. Salanne, R. Vuilleumier, P. A. Madden, C. Simon, P. Turq and B. Guillot, *J. Phys.: Condens. Matter*, 2008, **20**, 494207.
48 J. J. Molina, S. Lectez, S. Tazi, M. Salanne, J.-F. Dufrêche, J. Roques, E. Simoni, P. A. Madden and P. Turq, *J. Chem. Phys.*, 2011, **134**, 014511.
49 B. A. Bauer, T. R. Lucas, A. Krishtal, C. Van Alsenoy and S. Patel, *J. Phys. Chem. A*, 2010, **114**, 8984–8992.
50 B. Jeziorski, R. Moszynski and K. Szalewicz, *Chem. Rev.*, 1994, **94**, 1887–1930.
51 M. Masia, M. Probst and R. Ray, *Chem. Phys. Lett.*, 2006, **420**, 267–270.
52 A. Chaumont, R. Schurhammer and G. Wipff, *J. Phys. Chem. B.*, 2005, **109**, 18964–18973.
53 B. L. Bhargava and S. Balasubramanian, *J. Chem. Phys.*, 2007, **127**, 114510.
54 T. G. A. Youngs and C. Hardacre, *ChemPhysChem*, 2008, **9**, 1548–1558.
55 R. M. Lynden-Bell and T. G. A. Youngs, *J. Phys. Condens. Matter*, 2009, **21**, 424120.
56 A. Van der Vaart and K. M. Merz, *Int. J. Quantum Chem.*, 2000, **77**, 27–43.
57 O. Gálvez, P. C. Gómez and L. F. Pacios, *J. Chem. Phys.*, 2001, **115**, 11166–11184.
58 E. D. Glendening, *J. Phys. Chem. A*, 2005, **109**, 11936–11940.
59 R. Z. Khaliullin, A. T. Bell and M. Head-Gordon, *Chemistry: Eur. J.*, 2009, **15**, 851–855.
60 D. Boda, D. Gillespie, W. Nonner, D. Henderson and B. Eisenberg, *Phys. Rev. E*, 2004, **69**, 046702.